Fatigue delamination growth of composite laminates with fiber bridging: Theory and simulation

Lei Peng[1], Jifeng Xu[1,*]

[1] Beijing Aeronautical Science and Technology Research Institute, Beijing 102211, China
* Corresponding author: xujifeng@comac.cc

Abstract Mode I fatigue delamination growth rates and thresholds of composite laminates have been experimentally studied. Due to the fiber bridging generated across fracture interface, additional fracture resistance was found rising with crack growth, which make the traditional Paris law and threshold model unsuitable. Therefore, novel models taking the normalized strain energy release rate as fracture governing parameter were developed. The delamination resistance during fatigue crack growth caused by interface fracture and fiber bridging was totally evaluated by a new parameter namely fatigue delamination resistance G_{cf}. Excellent agreement with the experimental data was achieved by the normalized fatigue delamination growth rate and threshold models. Numerical simulation method for fatigue delamination was subsequently investigated. The fracture constitutive behavior with fiber bridging was defined by a tri-linear cohesive zone law, in which fatigue damage was introduced by a parameter available for both fracture and bridging zones. Development of the degradation law of the damage parameter is based on the normalized fatigue delamination models, enabling a direct link with experimental data. The simulation was implemented using user defined interface elements within finite element software ABAQUS.

Keywords Delamination, Fatigue crack growth, Cohesive zone, Damage degradation law, Composites

1. Introduction

Carbon fiber reinforced polymer composites are widely used in aircraft structures due to property advantages. Meanwhile, it brings design and analysis challenges caused by the ply-by-ply formulation of composites which is totally different from the traditional metal structures [1]. The failures in composite structures are mainly due to the defect, environment and out-of-plane sensitivities of the materials.

Delamination is one of the key factors for composites from damage initiation to final failures. The delamination growth behaviors have gained significant attention in the research communities in the past decade [2-7]. However, the delamination behavior of composites has not been completely understood under complex conditions, such as multidirectional interfaces, fatigue loading and fiber bridging case [8].

Linear elastic fracture mechanics is commonly utilized to study the interlaminar fracture of composites. Strain energy release rate (SERR) is accepted as the fracture governing parameter to evaluate interlaminar fracture toughness for composites rather than the stress intensity factor (SIF) for metals due to the simplicity of the calculation. Experimental studies and test methods for delamination resistance have been reviewed by Davies et al. [9] and Brunner et al. [10], numerical studies reviewed by Tay [11], respectively.

Multidirectional interface and fiber bridging are two important factors in real engineering applications, which bring significant influence on the interlaminar fracture of composite structures. As a summarized result from reports in literature [6, 12-14], multidirectional laminates always exhibit higher interlaminar fracture toughness, which is assumed to be caused by extrinsic toughening mechanisms such as blunted crack tips or deviation of the crack from the main crack plane to the adjacent layers and some in-ply energy absorption [15]. Fiber bridging could also bring considerable delamination resistance due to the energy absorbed in the bridging zone behind the

crack tip. For certain composite material systems, fiber bridging was found unavoidable and can be enhanced by multidirectional ply orientations [16]. Several laws [2, 17, 18] have been developed based on bridging zone model to evaluate the relationship between the fiber bridging stress and the crack tip opening displacement (CTOD). FEM cohesive element considering the fiber bridging effect was developed based on the bridging zone laws [19, 20].

For fatigue delamination propagation studies on composites, a Paris Law analogous linear log-log relationship between the fatigue crack growth rate and the SERR has been established by some significant fundamental works [21-26]. Fatigue degradation laws [27-30] based on cohesive interface elements and the Paris Law are developed to perform a numerical study and predict the fatigue crack growth by FEM programs. However, the Paris Law will become unsuitable for fiber bridging cases as the fatigue crack growth rate and threshold significantly affected by the additional delamination resistance. Remarkable R-curve effects on the fatigue delamination have been observed and analyzed by Hojo et al. [5] for Zanchor-reinforced laminates, Argülles et al. [31] for unidirectional laminates with fiber bridging and Shivakumar et al. [32] for woven/braided fiber composites. A bridging model was developed specially for fatigue delamination by Gregory and Spearing [33], finding that the scatter of crack propagation data was significantly reduced by applying the model.

A novel fatigue delamination resistance parameter was introduced by Peng et al. [8, 34, 35] to quantitatively evaluate the effect of R-curves on the fatigue delamination growth. Normalized fatigue crack growth rate and threshold model taking the ratio of SERR to the fatigue delamination resistance as the governing fracture parameter were subsequently developed. Excellent agreement with experiments was obtained by applying the models on experimental data from carbon/bismaleimide composite laminates.

Based on the normalized fatigue delamination model, the study presented here attempt to develop a numerical model to predict the fatigue delamination by interface elements. A tri-linear bridging zone model is adopted to simulate the fiber bridging effect. The normalized SERR is taken as the damage parameter to introduce fatigue damage by a degradation law. Numerical validation is performed by UMAT subroutine in commercial FEM software ABAQUS to show the ability of the model.

2. Model Description

2.1. Fatigue delamination growth model

A simple form of Paris Law for composites has developed by Wikins [36] and Singh and Greenhalgh [24], shown as:

$$\frac{\mathrm{d}a}{\mathrm{d}N} = A(\Delta G)^p \tag{1}$$

where da/dN is the propagation rate of delamination, ΔG the total SERR range in a fatigue cycle, A and p material constants.

For fiber bridging laminates, a normalized SERR was proposed instead to evaluate the effect of R-curve on the fatigue crack growth, express as:

$$g_{\max}(a) = \frac{G_{\max}(a)}{G_{\mathrm{cf}}(a)} \tag{2}$$

where $G_{cf}(a)$ is the fatigue delamination resistance, defined as the critical energy release rate during fatigue crack growth. The normalized Paris Law was thus reformed as:

$$\left(\frac{\mathrm{d}a}{\mathrm{d}N}\right)_a = C'(g_{\max}(a))^r \tag{3}$$

where C' and r are the new fatigue constants.

A normalized fatigue threshold parameter could also be proposed based on the fatigue delamination resistance, shown as:

$$g_{\mathrm{th}} = \frac{G_{\mathrm{th}}(a)}{G_{\mathrm{cf}}(a)} \tag{4}$$

2.2. Calculation of fatigue delamination resistance

The "compliance approach" [35] to obtain the fatigue delamination resistance, G_{cf}, is briefly introduced here. The approach is developed for fiber bridging cases and based on the following hypothesis: the delamination resistance of fatigue specimen is equal to the value of corresponding static specimen which exhibits the same force–displacement behavior. According to ''compliance approach'', the fatigue delamination resistance at certain crack length, a_1, could be determined by comparing the normalized compliance of fatigue and static specimens. The procedure was summarized in the following equation:

$$\begin{aligned} &\text{if } \frac{\bar{C}_{\mathrm{f}}(a_1)}{\bar{C}_{\mathrm{s}}(a_1)} - 1 < -\varepsilon_0 \\ &\quad G_{\mathrm{cf}}(a_1) = G_{\mathrm{c}}\left(a\Big|_{\bar{C}_{\mathrm{s}}(a)=\bar{C}_{\mathrm{f}}(a_1)}\right) \\ &\text{else} \\ &\quad G_{\mathrm{cf}}(a_1) = G_{\mathrm{c}}(a_1) \end{aligned} \tag{5}$$

where $\bar{C}$ is the normalized compliance of specimen, calculated by Eq. (6). ε_0 is the critical tolerance to consider experimental scatters of the compliance. The subscript "f" and "s" indicate the fatigue and static specimens, respectively.

$$\bar{C} = \frac{1}{m} bh^3 \tag{6}$$

where m is the slope of force-displacement curve of the specimen, b and h the width and half thickness, respectively.

2.3. Fiber bridging zone model

The mode I fiber bridging zone model is discussed here, as illustrated in Fig. 1. The SERR for double cantilever beam (DCB) specimen could be calculated using the equation below [37]:

$$G_{\mathrm{I}} = \frac{3Pd}{2b(a+\chi h)} \frac{F}{N'} \tag{7}$$

where F and N' are correction factor for large displacements and load-block effect, respectively. χ is a correction for crack tip displacement and rotation, which allows for the beam not being perfectly built in. Generally, χh value can be obtained experimentally by plotting the cubic root of compliance as a function of crack length and determining the intercept on the x-axies [38]. For fiber

bridging cases, however, the compliance could be reduced by the bridging fibers, which results in a larger wrong value of χ. According to [8], experimental data for the crack length within significant bridging zone should be excluded during the fitting procedure to get the correct χ value.

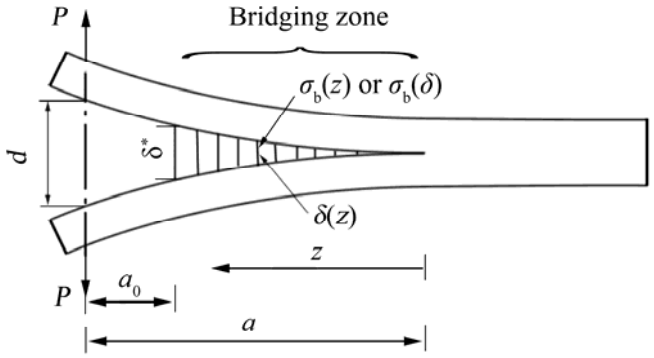

Figure 1. Illustration of fiber bridging zone for DCB specimen

A bridging zone model to calculate the bridging stress σ_b versus the CTOD δ was derived by Tamuzs et al. [18]:

$$G_c = \int_0^{\delta^*} \sigma_b(\delta)\mathrm{d}\delta + G_0 \tag{8}$$

where G_0 and G_c indicate the initial and total SERR, respectively. δ^* is the crack opening displacement at the pre-crack tip. The distribution of bridging stress could thus be experimentally determined by differentiating Eq. (8) with respect to δ^*.

2.4. Tri-linear interface element model

To simplify the numerical model, the fiber bridging behavior is described by a tri-linear constitutive law shown in Fig. 2, although the real function of bridging stress is nonlinear.

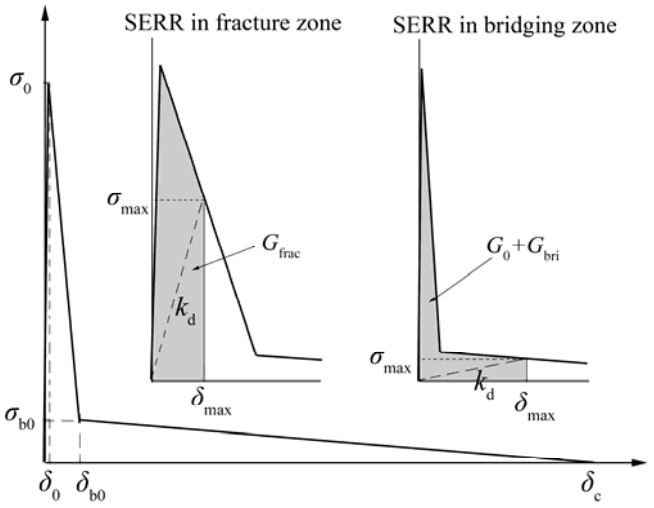

Figure 2. Illustration of the tri-linear cohesive constitutive law

The σ_0 and σ_{b0} in Fig. 2 indicate the strength at the start of fracture zone and bridging zone, respectively, while δ_0 and δ_{b0} indicate the corresponding displacement values. δ_c is the critical displacement for the final failure of the element. δ_{max} is the maximum displacement for the element being loaded and σ_{max} is the corresponding stress value. The constitutive relationship could thus be expressed as:

$$\sigma_{max} = \begin{cases} k_0 \delta_{max} & \text{for } \delta_{max} \le \delta_0 \\ \sigma_0 + \dfrac{\sigma_{b0} - \sigma_0}{\delta_{b0} - \delta_0}\left(\delta_{max} - \delta_0\right) & \text{for } \delta_0 < \delta_{max} \le \delta_{b0} \\ \sigma_{b0} - \dfrac{\sigma_{b0}}{\delta_c - \delta_{b0}}\left(\delta_{max} - \delta_{b0}\right) & \text{for } \delta_{b0} < \delta_{max} \le \delta_c \\ 0 & \text{for } \delta_{max} > \delta_c \end{cases} \tag{9}$$

where $k_0 = \sigma_0/\delta_0$, presents the initial stiffness. The stiffness of damaged element could thus be expressed as:

$$k_d = \frac{\sigma_{max}}{\delta_{max}} \tag{10}$$

The calculation of SERR is summarized as follows:

$$G_{max} = \begin{cases} \dfrac{1}{2}\sigma_{max}\delta_{max} & \text{for } \delta_{max} \le \delta_0 \\ \dfrac{1}{2}\left((\sigma_0 + \sigma_{max})\delta_{max} - \sigma_0\delta_0\right) & \text{for } \delta_0 < \delta_{max} \le \delta_{b0} \\ G_0 + \dfrac{1}{2}(\sigma_{max} + \sigma_{b0})(\delta_{max} - \delta_{b0}) & \text{for } \delta_{b0} < \delta_{max} \le \delta_c \\ G_T & \text{for } \delta_{max} > \delta_c \end{cases} \tag{11}$$

where the initial and total critical SERR (G_0 and G_T) have the expression shown as:

$$G_0 = \frac{1}{2}\left((\sigma_0 + \sigma_{b0})\delta_{b0} - \sigma_0\delta_0\right) \tag{12}$$

$$G_T = G_0 + \frac{1}{2}\left(\sigma_{b0}(\delta_c - \delta_{b0})\right) \tag{13}$$

2.5. Fatigue degradation law

The damage parameter of tri-linear cohesive element is defined by displacement as follows:

$$d = \frac{\delta_{max} - \delta_0}{\delta_{b0} - \delta_0} \tag{14}$$

From the expression, d has a value from 0 to 1 while the element in fracture zone has a value from 1 to $(\delta_c\text{-}\delta_0)/(\delta_{b0}\text{-}\delta_0)$ in bridging zone. This definition implies that the crack tip is at the end of fracture zone where d equal to 1, which is in accordance with the linear elastic fracture mechanics. For a tri-linear cohesive element, the damage is the sum of three parts:

$$d = d_s + d_f + d_b \tag{15}$$

where the subscript "s", "f" and "b" indicate quasi-static, fatigue and bridging damage, respectively.

Fig. 3 presents the illustration of the fatigue damage model of the tri-linear cohesive element to

simulate fatigue crack growth of DCB specimen. The fatigue damage is activated only in the fracture zone, which means the elements in bridging zone will not be degraded under cyclic loading. This hypothesis is supported by the experiment which shows that the damage in bridging zone under fatigue and static loading is equivalent for mode I delamination.

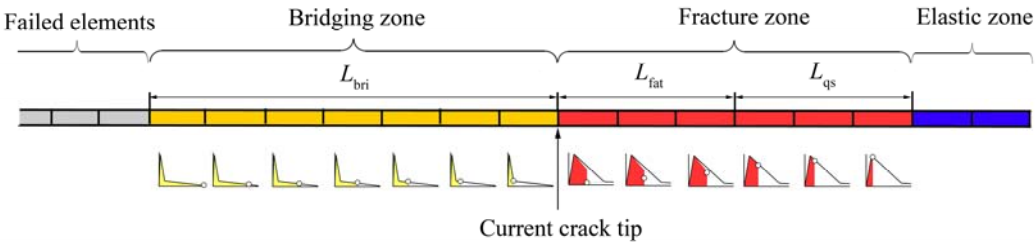

Figure 3. Damage of elements in fracture and bridging zones

A fatigue damage algorithm developed by Harper and Hallett [27] is used to link the fatigue crack growth law with the damage of cohesive elements, shown as:

$$\frac{\partial d_f}{\partial N} = \frac{1-d_s-d_{f,u}}{L_{fat}} \frac{\partial a}{\partial N} \tag{16}$$

where d_f and d_s are the fatigue and static damage, respectively. $d_{f,u}$ is the unwanted fatigue damage defined by an equivalent σ-δ response under fatigue loading. By estimating the fracture zone using the normalized SERR and assuming the fatigue damage length occupy half of fracture zone, the fatigue damage law is given:

$$\frac{\partial d_f}{\partial N} = \frac{1-d_s-d_{f,u}}{0.5\left(\frac{G_{max}}{G_0}\right)L_{cz,f}} \frac{\partial a}{\partial N} \tag{17}$$

where $L_{cz,f}$ is the fully developed numerical fracture zone length determined by a quasi-static analysis [27].

Once the total damage d reaches the value of 1, the fatigue degradation law is suppressed and the element enters the bridging zone.

3. Results

3.1. Bridging stress

The quasi-static and fatigue delamination growth law were determined by T700/QY811 carbon/bismaleimade unidirectional laminates. Details of the specimens and experiments could be found in the authors' previously published papers [1, 8, 35].

The bridging stress calculated from experimental data by Eq. (8) is presented in Fig. 4. The actual nonlinear σ_b-δ response is translated to the numerical response in dotted line, which ensures the total bridging energy are equivalent by making $G_A = G_B$.

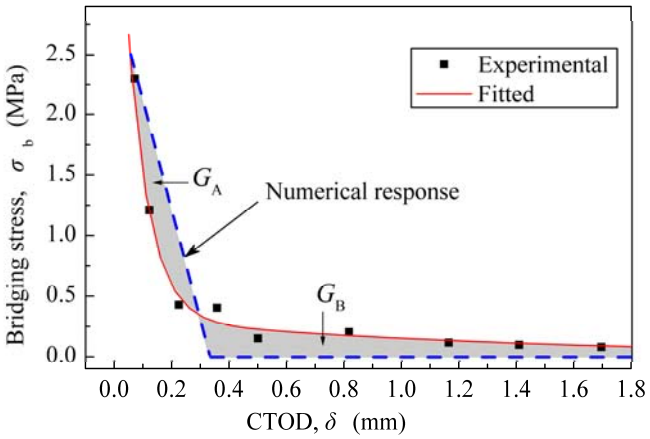

Figure 4. The experimental and numerical response between bridging stress and displacement

3.2. Fatigue crack growth rates and thresholds

The data reduction process of fatigue crack growth rates and thresholds could be found in [8]. The results are given in Fig. 5 here by applying the normalized law expressed in Eq. (2) to (4).

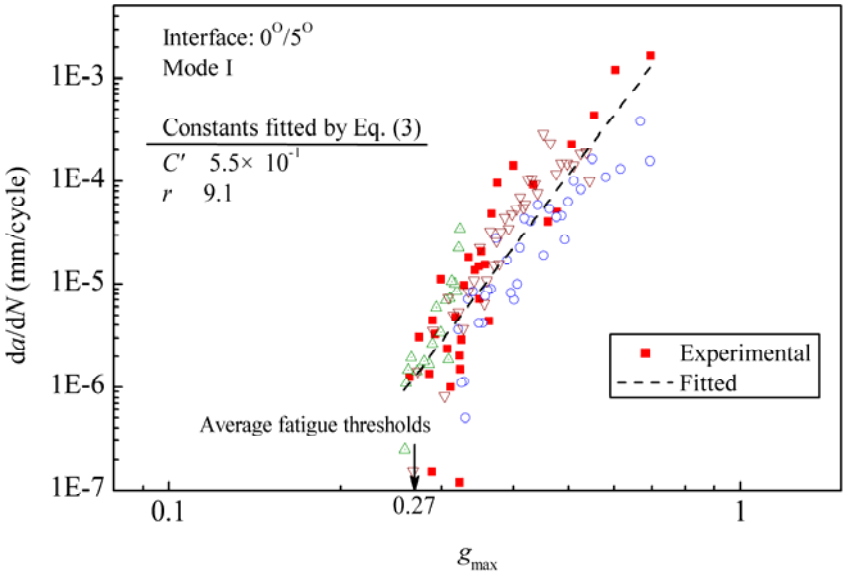

Figure 5. Experimentally obtained fatigue crack growth rates and thresholds

3.3. Numerical verification of tri-linear element

The UMAT subroutine in ABAQUS (v6.10) is used to verify the numerical model of tri-linear constitutive law. The laminate elastic properties from the tested specimens are as follows: E_{11} = 130 GPa, $E_{22} = E_{33}$ = 10.4 GPa, $G_{12} = G_{13}$ = 6.36 GPa, $\nu_{12} = \nu_{13}$ = 0.3. Interfacial properties to be input for the cohesive elements are: G_0 = 0.14 N/mm, G_c = 0.82 N/mm, σ_0 = 30 MPa, $k_0 = 1\times10^5$ N/mm^3. Varied bridging stress values from 0.5 to 2.5 are used following the rule in Section 3.1 to see the dependence of the model on bridging stresses.

The verification is performed on DCB specimen under quasi-static loading. The result of displacement-force relationship is presented in Fig. 6. The oscillations of numerical curves are caused by the large element size which was selected considering the computing size.

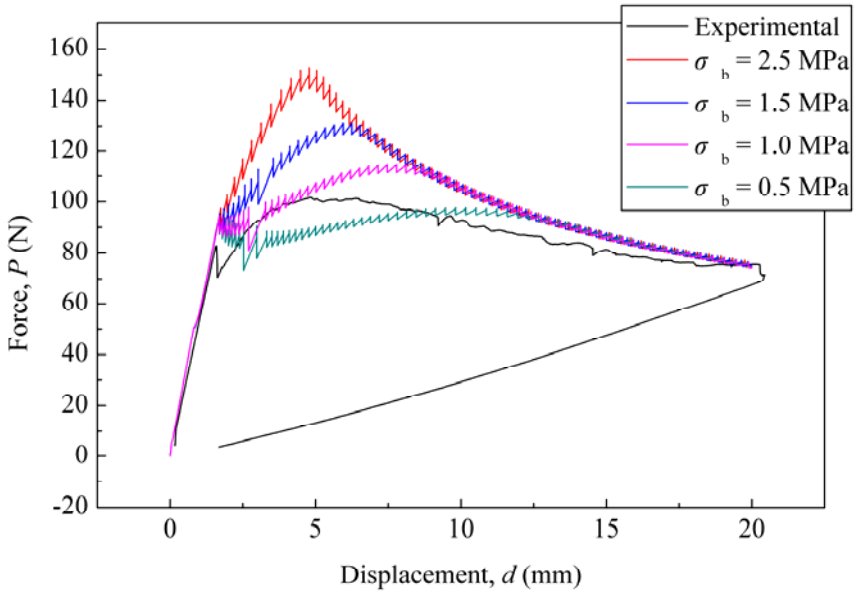

Figure 6. Force displacement response of DCB specimen from experiment and simulation

It is found that the value of bridging stress significantly affects the response of the specimen. Fig. 6 also implies that the linear law of σ_b-δ response doesn't fit the experiments very well. By making $G_A = G_B$ in Fig. 4, the determined σ_b distribution degrade the cohesive element too fast such as σ_b = 2.5 MPa in Fig. 6, or too slow as σ_b = 0.5 MPa in the figure.

4. Conclusion

The delamination growth behavior of composite laminates with fiber bridging is experimentally and numerically studied. A normalized fatigue crack growth rates law and thresholds model is presented to introduce the R-curve effect caused by fiber bridging. The cohesive element approach is also extended from bilinear constitutive response to a tri-linear response to simulate the delamination both in fracture and bridging zone.

The normalized fatigue law is found in accordance with experiments in high degree. The numerical model, however, degrades the cohesive element too fast or too slow due to the linear bridging stress law adopted. A nonlinear bridging law should be developed to fit the experiment better and a numerical verification for fatigue delamination growth will be conducted based on the new bridging law.

Acknowledgement

Financial support provided by the National High Technology Research and Development Program of China (863 Program) through grant number 2012AA040209, and by the National Natural Science Foundation of China through grant number 11202243 is gratefully acknowledged.

References

[1] L. Peng, J. Xu, J. Zhang and L. Zhao, Mixed mode delamination growth of multidirectional composite laminates under fatigue loading. Eng Fract Mech, 96 (2012) 676.
[2] L. Sorensen, J. Botsis, T. Gmür and L. Humbert, Bridging tractions in mode I delamination: Measurements and simulations. Compos Sci Technol, 68 (2008) 2350.
[3] A. J. Brunner, S. Stelzer, G. Pinter and G. P. Terrasi, Mode II fatigue delamination resistance of advanced fiber-reinforced polymer-matrix laminates: Towards the development of a standardized test procedure. Int J Fatigue, (2012).
[4] A. J. Brunner, N. Murphy and G. Pinter, Development of a standardized procedure for the characterization of interlaminar delamination propagation in advanced composites under fatigue mode I loading conditions. Eng Fract Mech, 76 (2009) 2678.
[5] M. Hojo, K. Nakashima, T. Kusaka, M. Tanaka, T. Adachi, T. Fukuoka and M. Ishibashi, Mode I fatigue delamination of Zanchor-reinforced CF/epoxy laminates. Int J Fatigue, 32 (2010) 37.
[6] J. Andersons and M. Köig, Dependence of fracture toughness of composite laminates on interface ply orientations and delamination growth direction. 64 (2004) 2139.
[7] B. D. Davidson, M. Kumar and M. A. Soffa, Influence of mode ratio and hygrothermal condition on the delamination toughness of a thermoplastic particulate interlayered carbon/epoxy composite. Composites Part A: Applied Science and Manufacturing, 40 (2009) 67.
[8] L. Peng, J. Zhang, L. Zhao, R. Bao, H. Yang and B. Fei, Mode I delamination growth of multidirectional composite laminates under fatigue loading. J Compos Mater, 45 (2011) 1077.
[9] P. Davies, B. R. K. Blackman and A. J. Brunner, Standard test methods for delamination resistance of composite materials: current status. Appl Compos Mater, 5 (1998) 345.
[10] A. J. Brunner, B. R. K. Blackman and P. Davies, A status report on delamination resistance testing of polymer-matrix composites. Eng Fract Mech, 75 (2008) 2779.
[11] T. E. Tay, Characterization and analysis of delamination fracture in composites - a review of developments from 1990 to 2001. Applied Mechanics Reviews, 56 (2003) 1.
[12] B. D. Davidson, R. D. Bialaszewski and S. S. Sainath, A non-classical, energy release rate based approach for predicting delamination growth in graphite reinforced laminated polymeric composites. Compos Sci Technol, 66 (2006) 1479.
[13] A. Quispitupa, C. Berggreen and L. A. Carlsson, On the analysis of a mixed mode bending sandwich specimen for debond fracture characterization. Eng Fract Mech, 76 (2009) 594.
[14] A. B. Pereira and A. B. de Morais, Mixed mode I + II interlaminar fracture of carbon/epoxy laminates. Composites Part A: Applied Science and Manufacturing, 39 (2008) 322.
[15] P. Naghipour, M. Bartsch, L. Chernova, J. Hausmann and H. Voggenreiter, Effect of fiber angle orientation and stacking sequence on mixed mode fracture toughness of carbon fiber reinforced plastics: Numerical and experimental investigations. Materials Science and Engineering: A, 527 (2010) 509.
[16] N. S. Choi, A. J. Kinloch and J. G. Williams, Delamination fracture of multidirectional carbon-fiber/epoxy composites under mode I, mode II and mixed-mode I/II loading. J Compos Mater, 33 (1999) 73.
[17] A. Szekrényes and J. Uj, Advanced beam model for fiber-bridging in unidirectional composite double-cantilever beam specimens. Engneering Fracture Mechanics, 72 (2005) 2686.
[18] V. Tamuzs, S. Tarasovs and U. Vilks, Progressive delamination and fiber bridging modeling in double cantilever beam composite specimens. Eng Fract Mech, 68 (2001) 513.
[19] J. Wang, Cohesive-bridging zone model of FRP-concrete interface debonding. Eng Fract Mech, 74 (2007) 2643.
[20] B. F. Søensen and T. K. Jacobsen, Characterizing delamination of fibre composites by mixed mode cohesive laws. Compos Sci Technol, 69 (2009) 445.

[21] M. Hojo, C. Gustafson, K. Tanaka and R. Hayashi, in Advanced Materials for Severe Service Applications (Tokyo, Japan, 1987) p. 353.
[22] N. Blanco, E. K. Gamstedt, L. E. Asp and J. Costa, Mixed-mode delamination growth in carbon-fibre composite laminates under cyclic loading. Int J Solids Struct, 41 (2004) 4219.
[23] L. E. Asp, A. Sjogren and E. S. Greenhalgh, Delamination growth and thresholds in a carbon/epoxy composite under fatigue loading. Journal of Composites Technology and Research, 23 (2001) 55.
[24] S. Singh and E. Greenhalgh, Mixed-mode delamination growth in carbon-fiber composites under fatigue loading, (Report DRA/SMC/CR961052/1.0 Defence Research Agency, 1996).
[25] A. Argüelles, J. Viña, A. Fernandez-Canteli, I. Viña and J. Bonhomme, Influence of the matrix constituent on mode I and mode II delamination toughness in fiber-reinforced polymer composites under cyclic fatigue. Mech Mater, 43 (2011) 62.
[26] M. Kenane, Z. Azari, S. Benmedakhene and M. L. Benzeggagh, Experimental development of fatigue delamination threshold criterion. Composites Part B: Engineering, 42 (2011) 367.
[27] P. W. Harper and S. R. Hallett, A fatigue degradation law for cohesive interface elements - Development and application to composite materials. Int J Fatigue, 32 (2010) 1774.
[28] S. Maiti and P. H. Geubelle, Cohesive modeling of fatigue crack retardation in polymers: Crack closure effect. Eng Fract Mech, 73 (2006) 22.
[29] P. Naghipour, M. Bartsch and H. Voggenreiter, Simulation and experimental validation of mixed mode delamination in multidirectional CF/PEEK laminates under fatigue loading. Int J Solids Struct, 48 (2011) 1070.
[30] A. Turon, J. Costa, P. P. Camanho and C. G. Davila, Simulation of delamination in composites under high-cycle fatigue. Compos Part A-Appl S, 38 (2007) 2270.
[31] A. Argüelles, J. Viña, A. F. Canteli, M. A. Castrillo and J. Bonhomme, Interlaminar crack initiation and growth rate in a carbon-fibre epoxy composite under mode-I fatigue loading. Compos Sci Technol, 68 (2008) 2325.
[32] K. N. Shivakumar, H. Chen, F. Abali, D. Le and C. Davis, A total fatigue life model for mode I delaminated composite laminates. International Journal of Fatigue, 28 (2006) 33.
[33] J. R. Gregory and S. M. Spearing, A fiber bridging model for fatigue delamination in composite materials. Acta Mater, 52 (2004) 5493.
[34] L. Peng, J. Zhang, R. Bao, H. Yang and B. Fei, Effect of ply orientation on the delamination growth in a laminated composite under cyclic loading: mode I, in "ICCS15" (Porto, Portugal, 2009).
[35] J. Zhang, L. Peng, L. Zhao and B. Fei, Fatigue Delamination Growth Rates and Thresholds of Composite Laminates under Mixed Mode Loading. Int J Fatigue, (2012).
[36] D. J. Wilkins, J. R. Eisenmann, R. A. Camin, W. S. Margolis and R. A. Benson, in Damage in Composite Materials, ASTM STP 775, edited by K. L. Reifsnider (American Society for Testing and Materials, 1982) p. 168.
[37] S. Hashemi, A. J. Kinloch and J. G. Williams, Mechanics and mechanisms of delamination in a poly(ether sulphone)--Fibre composite. Compos Sci Technol, 37 (1990) 429.
[38] S. Hashemi, A. J. Kinloch and J. G. Williams, Corrections needed in double-cantilever beam tests for assessing the interlaminar failure of fibre-composites. J Mater Sci Lett, 8 (1989) 125.